

The exact eigenfunctions and eigenvalues of a particle in a box obtained using Gaussian wavepacket dynamics

This article has been downloaded from IOPscience. Please scroll down to see the full text article.

1986 J. Phys. A: Math. Gen. 19 2559

(<http://iopscience.iop.org/0305-4470/19/13/021>)

View [the table of contents for this issue](#), or go to the [journal homepage](#) for more

Download details:

IP Address: 129.252.86.83

The article was downloaded on 31/05/2010 at 19:20

Please note that [terms and conditions apply](#).

The exact eigenfunctions and eigenvalues of a particle in a box obtained using Gaussian wavepacket dynamics

Jeffrey R Reimers^{†‡} and Eric J Heller[§]

[†] Department of Chemistry B014, University of California, San Diego, La Jolla, California 92093, USA

[§] Physics and Chemistry Departments BG-10, University of Washington, Seattle, Washington 98195, USA

Received 10 October 1985

Abstract. Exact eigenfunctions for a particle in a box are obtained using Gaussian wavepacket dynamics. The eigenfunctions are obtained by propagating, without approximation, an infinite set of Gaussian wavepackets that collectively satisfy the boundary conditions of the problem, being coherent states appropriate to this problem. The method of images is applied to enforce these boundary conditions. This technique may be applied to the quantum billiard problem whenever the particle is confined to any open or closed region that tessellates space, regardless of the dimension of the region. Also, it is shown that the use of frozen Gaussians along with the De Leon-Heller spectral quantisation method gives the exact solution for the one-dimensional problem as well as for the above multi-dimensional problems, provided the components of the momentum of the wavepackets are chosen at random.

1. Introduction

Only a few quantum mechanical problems are analytically solvable. This small set of solvable problems has become a cornerstone of modern physics. Techniques which are normally approximate obtain solid foundations by solving some of these problems exactly. A computational technique that approximately describes the vibrational evolution of polyatomic molecules is Gaussian wavepacket dynamics [1]. Its success is directly associated with its ability to solve, without approximation, two important problems: the particle in free space, and the molecule in a general harmonic potential. Here we show that this technique, when adapted to ensure that the appropriate boundary conditions are satisfied, gives exact results for another fundamental problem: the particle in a box, also known as the ‘quantum billiard’. This problem is a paradigm for a large number of physical and chemical problems [2]. In other papers, we have shown that this technique can be adapted to give the exact eigenfunctions [3] and rotational spectrum [4] of yet another fundamental problem: the two-dimensional rigid rotor.

In § 2 we consider the one-dimensional case, using the method of images [5] to construct a set of wavefunctions which vanish at the box boundaries, and these wavefunctions are shown in § 3 to be coherent states appropriate to this problem. The

[‡] Present address: Department of Theoretical Chemistry F11, University of Sydney, New South Wales 2006, Australia.

results are generalised in § 4 to include particles contained within any open or closed sub-region of n -dimensional space, provided the method of images can be used to establish the boundary conditions [6, 7]. Such a region is said to *canonically tessellate* space by reflection [8, 9], and it is the domain of a Coxeter group [10–13]. In § 5 the use of frozen Gaussians and the De Leon–Heller spectral quantisation method [14] is shown to give exact results for the one-dimensional problem, and § 6 considers the generalisation of this result to multi-dimensional boxes. This provides insight into the success of the De Leon–Heller spectral quantisation method at calculating numerical eigenfunctions [15].

2. The one-dimensional closed box

A single Gaussian wavepacket does not vanish at the box boundaries, but an infinite sum of such wavepackets can be forced to vanish there. Each wavepacket in such a sum has the same width, but the wavepackets all have different centres, and their phases may vary in sign. The centres and relative phases are determined by the method of images, a technique introduced by Thomson [5] to ensure that the electrostatic potential arising from a point charge vanished at every point on a grounded conducting surface. It is directly applicable to eigenfunction problems [7]. An example set of wavepackets is given in figure 1, where the open and closed circles mark the centres of the Gaussian wavepackets and denote their sign. This box has length a and has its boundaries at positions $q = 0$ and $q = a$. Exactly one wavepacket centre is within the box at any given instant, and this wavepacket has images (wavepackets with alternate sign) located equidistantly from both box boundaries. These image wavepackets themselves have images, found by reflecting about the box boundaries. One of these reflections regenerates the original wavepacket, and this is said to be an *improper* image, while the other reflection generates a distinct (*proper*) image. The generation process is repeated *ad infinitum*, dividing space into regions which replicate the original box, each region containing exactly one wavepacket. No proper images lie in the original box, and the wavefunction is periodic with period $2a$.



Figure 1. A possible location for the centre of a Gaussian wavepacket and its images for a particle in a one-dimensional box of length a . Bold lines indicate the boundaries of the box. The open and closed circles indicate the relative phase of the wavepackets.

Let $|\psi_{q_i, p_i}\rangle$ be a normalised, coherent state Gaussian wavepacket, which, at time t , is centred at position q_i and momentum p_i . We can express this wavepacket in the position representation as

$$\psi_{q_i, p_i}(q) = \langle q | \psi_{q_i, p_i} \rangle = \exp\left\{ \frac{i}{\hbar} [\alpha_i (q - q_i)^2 + p_i (q - q_i) + \gamma_i] \right\} \tag{2.1}$$

or in the momentum representation as

$$\psi_{q_i, p_i}(p) = \langle p | \psi_{q_i, p_i} \rangle = (-2i\alpha_i)^{-1/2} \exp\left\{ \frac{i}{\hbar} [(4\alpha_i)^{-1} (p - p_i)^2 - q_i p + \gamma_i] \right\} \tag{2.2}$$

where α_t and γ_t are the width and phase of the Gaussian wavepacket, respectively, and $\text{Im } \alpha_t > 0$. These two representations of $|\psi_{q_t, p_t}\rangle$ are related by the Fourier transform

$$\psi_{q_t, p_t}(q) = (2\pi\hbar)^{-1/2} \int_{-\infty}^{\infty} dp e^{iap/\hbar} \psi_{q_t, p_t}(p) \tag{2.3}$$

which can also be written as

$$\psi_{-q_t, -p_t}(q) = (2\pi\hbar)^{-1/2} \int_{-\infty}^{\infty} dp e^{-iap/\hbar} \psi_{q_t, p_t}(p). \tag{2.4}$$

The wavefunction depicted in figure 1 is written as

$$|\Psi_{q_t, p_t}\rangle = \sum_{n=-\infty}^{\infty} (|\psi_{q_t+2na, p_t}\rangle - |\psi_{-q_t-2na, -p_t}\rangle) \tag{2.5}$$

and is composed of two equally spaced sets of identical wavepackets, each set moving in opposite directions.

As the Hamiltonian operator H is linear, the effect of the propagation

$$|\Psi_{q_t, p_t}\rangle = e^{-iHt/\hbar} |\Psi_{q_0, p_0}\rangle \tag{2.6}$$

can be written as

$$|\Psi_{q_t, p_t}\rangle = \sum_{n=-\infty}^{\infty} e^{-iHt/\hbar} (|\psi_{q_t+2na, p_t}\rangle - |\psi_{-q_t-2na, -p_t}\rangle) \tag{2.7}$$

where, for a particle in a box,

$$H = p^2/(2M) \tag{2.8}$$

and M is the mass of the particle. Thus, the time dependence of $|\Psi_{q_t, p_t}\rangle$ is given by the sum of the time dependences of the individual wavepackets, and, as these wavepackets behave like a particle in free space, Gaussian wavepacket dynamics [1] propagates these wavepackets without approximation. The widths and phases of each individual wavepacket change in unison, while the momenta and relative positions of the centres of the two sets of wavepackets do not change at all. Note that no special action is required when one of the wavepackets passes through a boundary as an image wavepacket simultaneously enters the box, keeping the value of $|\Psi_{q_t, p_t}\rangle$ zero at the boundary. From the point of view of an observer inside the box, the wavepacket appears to be elastically reflected from the box wall.

The eigenvalues are obtained from the power spectrum

$$I(\omega) = (2\pi)^{-1/2} \int_{-\infty}^{\infty} e^{i\omega t} dt \langle \Psi_{q_0, p_0} | \Psi_{q_t, p_t} \rangle. \tag{2.9}$$

This Fourier transform produces a set of δ functions with energies E_m and 'intensities' I_m , and the corresponding eigenfunctions are given by

$$|\chi_m\rangle = N_m \int_{-\infty}^{\infty} e^{iE_m t/\hbar} dt |\Psi_{q_t, p_t}\rangle \tag{2.10}$$

where N_m is a normalising constant. The spatial dependence of these eigenstates, $\chi_m(q) = \langle q | \chi_m \rangle$, can be obtained by writing the wavepackets in the momentum representation. Using (2.2)-(2.4) and (2.6), (2.10) is written as

$$\begin{aligned} \chi_m(q) \propto & \int_{-\infty}^{\infty} e^{iE_m t/\hbar} dt \left(e^{-iHt/\hbar} \sum_{n=-\infty}^{\infty} \psi_{q_i+2na, p_i}(q) - \psi_{-q_i-2na, -p_i}(q) \right) \\ & \int_{-\infty}^{\infty} dp \left\{ \int_{-\infty}^{\infty} dt \exp \left[\frac{it}{\hbar} \left(E_m - \frac{p^2}{2M} \right) \right] \right\} \psi_{q_0, p_0}(p) \\ & \times \sin \left(\frac{qp}{\hbar} \right) \sum_{n=-\infty}^{\infty} \exp \left(\frac{-2nai p}{\hbar} \right) \end{aligned} \tag{2.11}$$

and the summation can be non-zero only when

$$p = m\pi\hbar/a \tag{2.12}$$

for integer m , so that the time integral can be non-zero only when

$$E_m = (m\pi\hbar)^2/2Ma^2 \tag{2.13}$$

and thus the normalised eigenfunctions are

$$\chi_m(q) = (2/a)^{1/2} \sin(\pi mq/a). \tag{2.14}$$

These eigenfunctions have nodes at the box boundaries $q=0$ and $q=a$, and (2.12)-(2.14) are generally known as the solutions to the problem of a particle in a closed one-dimensional box [16].

The wavefunctions generated by a freely moving Gaussian wavepacket are the free particle wavefunctions e^{ikq} . Because each set of Gaussians comprising $|\Psi_{q_i, p_i}\rangle$ is periodic with period $2a$, the problem is quantised and admits solutions with particular values of k only. Finally, as the two sets of Gaussians are travelling in opposite directions, the plane waves produced by each set interfere, with the result that the final eigenfunctions, (2.14), are sine functions. Many of these properties have a counterpart in the problem of a two-dimensional rigid rotor [3].

Note that the particle in a closed box has energy levels which can be expressed as some subset of the integers times a number λ , where, in this case, $\lambda = \pi^2 \hbar^2 (2Ma^2)^{-1}$. As a consequence, all dynamics must be periodic and have the period $2\pi/\lambda = 4Ma^2/(\pi\hbar)$, independent of the momentum of the trajectory, p_0 .

This wavepacket technique also gives the exact eigenstates for a particle in both fully and partially open boxes. The fully open box is actually a particle in free space, and this problem is solved by just a single wavepacket [1], while the half-open box requires just one wavepacket and its mirror image.

3. The wavefunctions $|\Psi_{q_i, p_i}\rangle$ as coherent states

These wavefunctions share many of the attractive properties possessed by the coherent states of harmonic oscillators and of radiation [17], and can be regarded as coherent states appropriate to a particle in a box. Let us expand $|\Psi_{q_0, p_0}\rangle$ in terms of the eigenstates $|\chi_m\rangle$ as

$$|\Psi_{q_0, p_0}\rangle = \sum_{m=1}^{\infty} c_{p_0, q_0, m} |\chi_m\rangle \tag{3.1}$$

where

$$c_{p_0, q_0, m} = \langle \chi_m | \Psi_{q_0, p_0} \rangle = \left(\frac{-8\pi\hbar \operatorname{Im} \alpha_0}{a^2 \alpha_0^2} \right) \exp\left(\frac{-ip_0^2}{4\alpha_0\hbar} - \frac{i\hbar\pi^2 m^2}{4a^2 \alpha_0} \right) \sin\left[\frac{\pi m}{a} \left(q_0 - \frac{p_0}{2\alpha_0} \right) \right]. \tag{3.2}$$

This leads to an inner product relationship characteristic of coherent states:

$$\begin{aligned} (2\pi\hbar)^{-1} \int_0^a dq_0 \int_{-\infty}^{\infty} dp_0 c_{p_0, q_0, m} c_{p_0, q_0, n}^* &= \left(\frac{2}{\pi\hbar A a^2} \right)^{1/2} \int_{-\infty}^{\infty} dp_0 \exp\left[\frac{-p_0^2}{2\hbar A} - \frac{i\hbar\pi^2}{4a^2} \left(\frac{m^2}{\alpha_0} - \frac{n^2}{\alpha_0^*} \right) \right] \\ &\times \int_0^a dq_0 \sin\left[\frac{\pi m}{a} \left(q_0 - \frac{p_0}{2\alpha_0} \right) \right] \sin\left[\frac{\pi n}{a} \left(q_0 - \frac{p_0}{2\alpha_0^*} \right) \right] \\ &= \delta_{mn} A^{-1/2} \int_{-\infty}^{\infty} dp_0 \exp\left(\frac{-ip_0^2}{2\hbar A} - \frac{\hbar\pi^2 m^2}{2a^2 A} \right) \cos\left(\frac{i\pi m p_0}{aA} \right) \\ &= \delta_{mn} \end{aligned} \tag{3.3}$$

where $A = |\alpha_0|^2 / \operatorname{Im} \alpha_0$. Although (3.3) is tantamount to the completeness relation

$$1 = (2\pi\hbar)^{-1} \int_{-\pi}^{\pi} dq_0 \int_{-\infty}^{\infty} dp_0 |\Psi_{q_0, p_0}\rangle \langle \Psi_{q_0, p_0}| \tag{3.4}$$

one may also derive (3.4) by expanding

$$|X\rangle = \left(\int_{-\pi}^{\pi} dq_0 \int_{-\infty}^{\infty} dp_0 |\Psi_{q_0, p_0}\rangle \langle \Psi_{q_0, p_0}| \right) |\Psi_{q_1, p_1}\rangle$$

in terms of the eigenfunctions $|\chi_m\rangle$ using (3.2), then invoking the orthonormality of the eigenfunctions to deduce that

$$|X\rangle = \sum_{m=-\infty}^{\infty} \sum_{m'=-\infty}^{\infty} \left(\int_{-\pi}^{\pi} dq_0 \int_{-\infty}^{\infty} dp_0 c_{\phi_0, l_0, m} c_{\phi_0, l_0, m'}^* \right) c_{\phi_1, l_1, m'} |\chi_m\rangle$$

which simplifies using the inner product relation and (3.2) to produce

$$|X\rangle = 2\pi\hbar |\Psi_{q_1, p_1}\rangle$$

thus implying (3.4). A simple inverse to (3.1) exists and is determined by using $c_{\phi_0, l_0, m} = \langle \chi_m | \Psi_{q_0, p_0} \rangle$ to expand

$$\int_{-\pi}^{\pi} dq_0 \int_{-\infty}^{\infty} dp_0 c_{\phi_0, l_0, m} \langle \Psi_{q_0, p_0} | = \langle \chi_m | \left(\int_{-\pi}^{\pi} dq_0 \int_{-\infty}^{\infty} dp_0 |\Psi_{q_0, p_0}\rangle \langle \Psi_{q_0, p_0}| \right)$$

which, using the completeness relation, simplifies to

$$|\chi_m\rangle = (2\pi\hbar)^{-1} \int_{-\pi}^{\pi} dq_0 \int_{-\infty}^{\infty} dp_0 c_{\phi_0, l_0, m}^* |\Psi_{q_0, p_0}\rangle. \tag{3.5}$$

Other important properties of coherent states concern expressions for the traces of operators. If O is any operator, then

$$\operatorname{Tr}(O |\Psi_{q_0, p_0}\rangle \langle \Psi_{q_0, p_0}|) = \langle \Psi_{q_0, p_0} | O | \Psi_{q_0, p_0} \rangle \tag{3.6}$$

a result verified by expanding the trace in terms of the eigenstates [18]. Using the completeness relation (3.4), the trace of O itself may be expanded as

$$\text{Tr}(O) = (2\pi\hbar)^{-1} \text{Tr} \left(\int_{-\pi}^{\pi} dq_0 \int_{-\infty}^{\infty} dp_0 O |\Psi_{q_0, p_0}\rangle \langle \Psi_{q_0, p_0}| \right) \quad (3.7)$$

and this simplifies using (3.6) to give

$$\text{Tr}(O) = (2\pi\hbar)^{-1} \int_{-\pi}^{\pi} dq_0 \int_{-\infty}^{\infty} dp_0 \langle \Psi_{q_0, p_0} | O | \Psi_{q_0, p_0} \rangle. \quad (3.8)$$

This result is very useful and allows the high temperature formalism of Reimers *et al* [19] to be applied to directly calculate thermally averaged properties such as absorption spectra.

4. Generalisation to higher dimensions

This method applies to a particle confined to any region of an n -dimensional space that tessellates [8, 10] the space by reflection. Such a region, when continuously reflected about one of its boundary surfaces, covers all of the space evenly, and no proper image of the region lies within the region. It is referred to as an *image domain* [7], and closed image domains are examples of Coxeter groups [10–13]. Analytic eigenfunctions have been determined by Terras and Swanson [7] for all two- and three-dimensional regions that may be treated by this method, and other authors have treated some of these problems in detail [11, 12, 20–25]. Regions of higher dimension may also be treated, invoking results from the theory of Coxeter groups to prove that the method of images actually fulfils the boundary conditions. Note that this method cannot be applied, without approximation, to calculate eigenfunctions for systems for which, as yet, only numerical eigenfunctions have been obtained [15, 26–31].

An example of a closed two-dimensional image domain, a square, is given in figure 2, along with some nearby images of this domain formed by reflecting the square about its sides. The open and closed circles represent a possible set of centres for the Gaussian wavepackets as well as their relative phases, while the diagonal lines indicate a possible time history: as each wavepacket behaves like a particle in free space, the centres move in straight lines. When one of these wavepackets leaves a region, an image wavepacket simultaneously enters that region, ensuring that the value of the total wavefunction remains zero along the boundary. The new wavepacket appears, to an observer inside the box, to be the reflection of the original wavepacket: this result is a consequence of the Riemann–Schwarz reflection principle [9, 32]. Sketches of all of the two- and three-dimensional image domains solvable by this technique have been given by Terras and Swanson [6, 7].

5. The De Leon–Heller spectral quantisation method applied to a 1D box

This technique [14], based upon classical trajectories, determines approximate vibrational eigenstates of polyatomic molecules. It uses the frozen Gaussian approximation [33] to propagate the Gaussian wavepackets, and here we apply it to the problem of a particle in a one-dimensional box. First, the frozen (fixed width) Gaussians are propagated, producing the wavefunction $|\Psi_{q_t, p_t}^{FG}\rangle$ and the overlap $\langle \Psi_{q_0, p_0} | \Psi_{q_t, p_t}^{FG} \rangle$. The

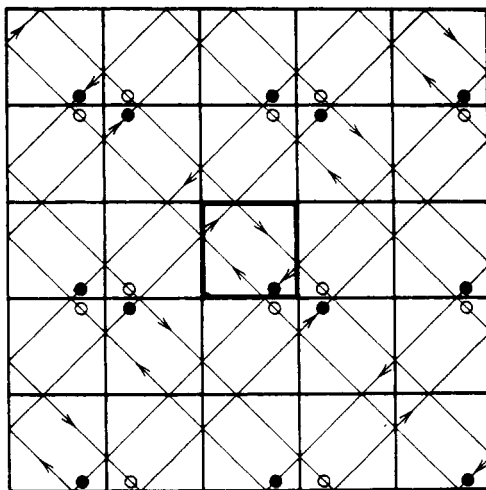


Figure 2. A possible location for the centre of a Gaussian wavepacket and its images for a particle in a two-dimensional square box. Bold lines indicate the boundaries of the box, and the diagonal arrows indicate a possible set of trajectories for the wavepackets. The open and closed circles indicate the relative phase of the wavepackets.

second and third steps apply (2.9) and (2.10) to determine a set of energy levels, E_m^{FG} , and wavefunctions, $|\chi_m^{FG}\rangle$, respectively. In the fourth step, more accurate energy levels $E_m^{FG'}$ are calculated using

$$E_m^{FG'} = \langle \chi_m^{FG} | H | \chi_m^{FG} \rangle. \tag{5.1}$$

Frozen Gaussians are not solutions of the time-dependent Schrödinger equation

$$i\hbar \frac{\partial |\Psi_{q_n, p_t}\rangle}{\partial t} = H |\Psi_{q_n, p_t}\rangle \tag{5.2}$$

but in one dimension they differ by only a phase factor from the solutions $|\Psi'_{q_n, p_t}\rangle$ of another wave equation, namely

$$-\frac{M^2}{p_0^2} \frac{\partial^2 |\Psi'_{q_n, p_t}\rangle}{\partial t^2} = H |\Psi'_{q_n, p_t}\rangle. \tag{5.3}$$

Any sum of functions f of the form $f(q \pm p_0 t / M)$ is a solution to this equation. Solving the equations of motion of a frozen Gaussian [33] shows that its centre moves in accordance with Hamilton's equations of motion

$$q_t = q_0 \pm p_0 t / M \quad p_t = p_0. \tag{5.4}$$

The frozen Gaussian constraint is

$$\alpha_t = \alpha_0 \quad \text{Re } \alpha_0 = 0, \text{Im } \alpha_0 > 0 \tag{5.5}$$

so that the frozen Gaussian wavepackets $|\Psi_{q_n, p_t}^{FG}\rangle$ differ from $|\Psi'_{q_n, p_t}\rangle$ by only the phase factor [33] $e^{i\gamma_t/\hbar}$,

$$|\Psi_{q_n, p_t}^{FG}\rangle = e^{i\gamma_t/\hbar} |\Psi'_{q_n, p_t}\rangle \tag{5.6}$$

where

$$\gamma_t = -\hbar \text{Im } \alpha_0 t / M + p_0^2 t / (2M). \tag{5.7}$$

This phase factor displaces the energy levels calculated using (2.9) and these levels are given by

$$E_m^{FG} = E'_m + \hbar \operatorname{Im} \alpha_0 / M - p_0^2 / (2M) \tag{5.8}$$

where m is an integer and

$$E'_m = m\pi\hbar p_0 / (aM) \tag{5.9}$$

are the energies that result when (5.3) is solved exactly. The ‘intensities’ of these lines are given from (2.9) as

$$I_m \propto \exp\left(\frac{-m^2\pi^2\hbar}{2a^2 \operatorname{Im} \alpha_0}\right) \left[\exp\left(\frac{m\pi p_0}{a \operatorname{Im} \alpha_0}\right) - 1 \right]. \tag{5.10}$$

Note that for $m=0$, the intensities arising from the oppositely moving sets of wavepackets completely cancel each other, and that the lines on the side of this line corresponding to negative values of mp_0 have negative intensities.

The eigenfunctions calculated from (2.10) are not affected by the phase factor $e^{i\nu}$, and as a result $|\chi_m^{FG}\rangle = |\chi'_m\rangle$, the stationary solutions to (5.3). It might seem to be small comfort that the frozen Gaussian dynamics satisfies the wrong wave equation; however, it is easy to see that both (5.2) and (5.3) share the same eigenfunctions. $|\Psi_{q_n, p_t}\rangle$ may be expanded, using (2.6) and (3.1), as a sum of products of time-dependent and time-independent functions

$$|\Psi_{q_n, p_t}\rangle = \sum_{m=-\infty}^{\infty} c_{q_0, p_0, m} e^{-iE_m t / \hbar} |\chi_m\rangle. \tag{5.11}$$

This function is a solution of the time-dependent Schrödinger equation if and only if

$$H|\chi_m\rangle = E_m|\chi_m\rangle \tag{5.12}$$

thus identifying $|\chi_m\rangle$ as the eigenfunctions of the Hamiltonian. Similarly, $|\Psi'_{q_n, p_t}\rangle$ may be expanded as

$$|\Psi'_{q_n, p_t}\rangle = \sum_{m=-\infty}^{\infty} c'_{q_0, p_0, m} e^{-iE'_m t / \hbar} |\chi'_m\rangle. \tag{5.13}$$

and this function is a solution to (5.3) if and only if

$$H|\chi'_m\rangle = \frac{M(E'_m)^2}{2p_0^2} |\chi'_m\rangle. \tag{5.14}$$

Thus $|\chi'_m\rangle$ are also the eigenfunctions of the Hamiltonian so that $|\chi_m\rangle = |\chi'_m\rangle$, $c'_{q_0, p_0, m} = c_{q_0, p_0, m}$, and

$$E_m = \frac{M(E'_m)^2}{2p_0^2} = \frac{M}{2p_0^2} \left(E_m^{FG} + \frac{p_0^2}{2M} - \frac{\hbar \operatorname{Im} \alpha_0}{M} \right)^2. \tag{5.15}$$

Finally, it follows from these relations, (5.7)–(5.9) and (5.13), that

$$|\Psi_{q_n, p_t}^{FG}\rangle = \sum_{m=-\infty}^{\infty} c_{q_0, p_0, m} e^{-iE_m^{FG} t / \hbar} |\chi_m\rangle \tag{5.16}$$

and thus the solutions $|\Psi_{q_n, p_t}\rangle$, $|\Psi'_{q_n, p_t}\rangle$ and $|\Psi_{q_n, p_t}^{FG}\rangle$ all share the same expansion coefficients $c_{q_0, p_0, m}$ and eigenfunctions $|\chi_m\rangle$. Their dynamics is different only because the eigenvalues differ, causing the eigenfunctions to dephase at different rates. Thus, by Fourier transforming, using (2.10), at the frequencies E_m^{FG} , the *exact* eigenfunctions

of the Schrödinger equation can be extracted from the 'approximate' frozen Gaussian dynamics. Noting that $|\chi_m\rangle = |\chi_m^{FG}\rangle$, we see that $E_m^{FG} = E_m$, and the true eigenvalues can be extracted using either (5.1) or (5.15).

The above argument presents a simple physical picture for why the frozen Gaussians produce the exact eigenstates for a particle in a one-dimensional box. This picture is extended in other papers [3, 34] to provide an *a posteriori* justification for the use of the De Leon–Heller spectral quantisation method to determine the vibrational eigenstates of polyatomic molecules. There too, frozen Gaussian dynamics provides a poor description of the motion of wavepackets under the Schrödinger equation, but again they provide a good approximation to the dynamics of a different differential equation which shares its eigenfunctions with the Schrödinger equation.

Unfortunately, the argument presented in this section cannot easily be generalised to describe particles in boxes of more than one dimension. This arises as there is only one proportionality constant present in (5.3) while each degree of freedom demands its own constant in order for the argument to generalise. One can find, however, an alternative interpretation of the mathematics that does allow these results to be extended. Each wavepacket in the sum (2.7) can be regarded as being a wavepacket propagating in free space, and frozen Gaussians are known to produce the exact eigenstates for particles in free space: plane waves. Adding all of the plane waves travelling in the same direction quantises the solutions, and only those plane waves with the correct periodicity remain. These plane waves are in fact the eigenstates of a particle on a ring of circumference $2a$ [3], but for a particle in a box there exists an additional set of wavepackets travelling in the opposite direction, and the two sets of generated plane waves interfere making the final solutions, (2.14), sine functions. Thus we see that the frozen Gaussians produce plane waves, and that the plane waves combine to give the eigenstates. This approach may be extended to higher dimensions as it is known that, in general, eigenstates may be expressed in terms of sums of plane waves [7, 12, 21–23].

6. Extension of the De Leon–Heller method to higher dimensions

The use of frozen Gaussians does not provide, in general, the exact solutions for a particle in a box of more than one dimension. While each component of a separable multi-dimensional frozen Gaussian wavepacket satisfies (5.3), the product wavepacket does not satisfy the multi-dimensional generalisation of (5.3). An example of a trajectory that, using frozen Gaussians, does not lead to the correct eigenstates is given in figure 2: this is a periodic trajectory and the motion resembles the 1:1 Lissajous figure [35]. Along the path of motion the desired plane waves are in fact generated, but at points not on this trajectory the wavefunction calculated from (2.10) is just a sum of Gaussians, not the exact eigenstates. For rectangular boxes, any trajectory for which $a_x p_{y0} / a_y p_{x0}$ is a rational number, where a_x and a_y are the box lengths and p_{x0} and p_{y0} are the components of the momenta, will give rise to a periodic trajectory and (2.10) will not produce the eigenstates. An example of a trajectory which is not periodic is given in figure 3, where we choose, in dimensionless units defined so that $\hbar = M = a_x = 1$, $a_y = 1$, $p_{x0} = 1 + 5^{1/2}$ and $p_{y0} = 2$ so that $a_x p_{y0} / a_y p_{x0}$ is irrational. After an infinite amount of time, this trajectory covers all space evenly [35], and every point in position space lies on the trajectory. The four distinct directions of travel give rise to four sets of plane waves and these interfere to produce the exact eigenstates.

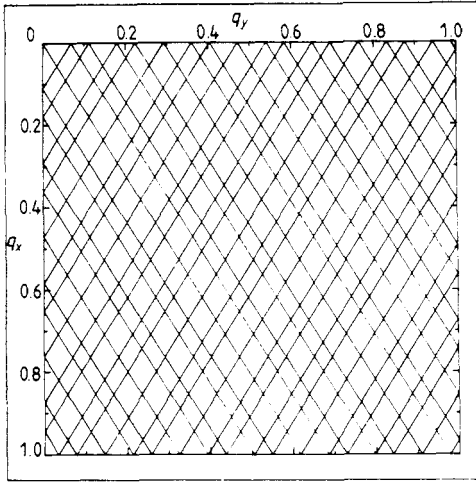


Figure 3. The extract $0 \leq t \leq 10.2$ taken from the non-periodic trajectory with $a_x = a_y = 1$, $p_x = 1 + 5^{1/2}$ and $q_{x0} = q_{y0} = 0$. This trajectory is not plotted up to $t = 75$ as the square would be completely shaded by this pen.

Consider the separable, multi-dimensional frozen Gaussian wavepacket defined as the product

$$|\psi_{q_{xt}, p_{xt}}^{(x)}\rangle |\psi_{q_{yt}, p_{yt}}^{(y)}\rangle \tag{6.1}$$

of functions of the form of (2.1), where q_x and q_y are the position variables whose expectation values at time t are

$$q_{xt} = q_{x0} + p_{x0}t/M \quad q_{yt} = q_{y0} + p_{y0}t/M \tag{6.2}$$

respectively, and q_{x0} and q_{y0} are the initial expectation values of position. Using the method of images, a wavefunction with the correct boundary properties can be written as

$$\sum_{n_x=-\infty}^{\infty} \sum_{n_y=-\infty}^{\infty} |\psi_{q_{xt}+2n_x a_x, p_{xt}}^{(x)}\rangle |\psi_{q_{yt}+2n_y a_y, p_{yt}}^{(y)}\rangle - |\psi_{q_{xt}+2n_x a_x, p_{xt}}^{(x)}\rangle |\psi_{-q_{yt}-2n_y a_y, -p_{yt}}^{(y)}\rangle \\ - |\psi_{-q_{xt}-2n_x a_x, -p_{xt}}^{(x)}\rangle |\psi_{q_{yt}+2n_y a_y, p_{yt}}^{(y)}\rangle + |\psi_{-q_{xt}-2n_x a_x, -p_{xt}}^{(x)}\rangle |\psi_{-q_{yt}-2n_y a_y, -p_{yt}}^{(y)}\rangle. \tag{6.3}$$

Under frozen Gaussian dynamics, substitution of this wavefunction into (2.9) gives a spectrum which is a convolution of the spectra for the individual x and y components,

$$E_m = \frac{2\hbar \text{Im } \alpha_0}{M} - E + \frac{\pi\hbar}{M} \left(\frac{m_x p_{x0}}{a_x} + \frac{m_y p_{y0}}{a_y} \right) \tag{6.4}$$

where $\mathbf{m} = (m_x, m_y)$ is a vector of the quantum numbers, and E is the classical energy of the trajectory

$$E = (2M)^{-1} (p_{x0}^2 + p_{y0}^2). \tag{6.5}$$

The energy spectrum calculated from the trajectory shown in figure 3, extended to over seven times its length, is given in figure 4, along with the spectrum obtained using thawed Gaussian dynamics from just the portion of the trajectory shown. Note that frozen Gaussian spectra are purely real only if the trajectory starts at a box corner,

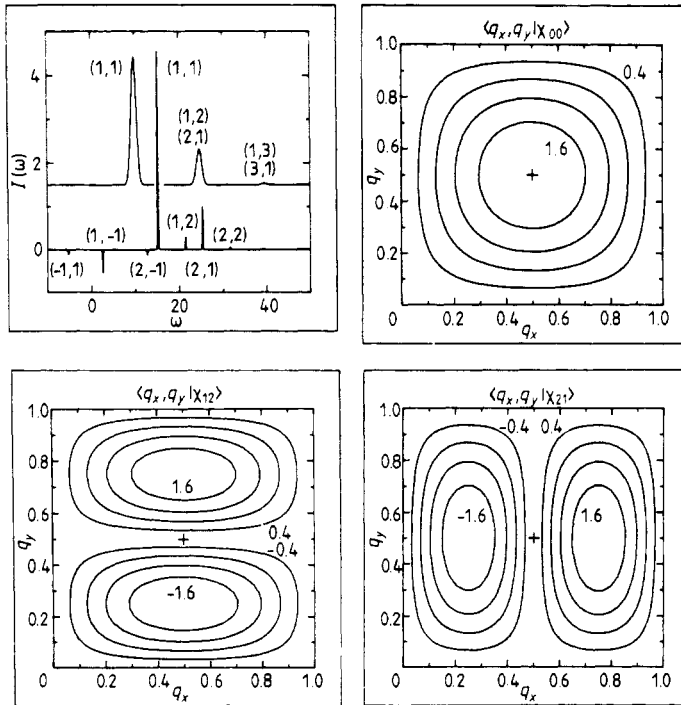


Figure 4. In the top left corner is the power spectrum obtained using thawed Gaussians from the trajectory given in figure 3, as well as the power spectrum obtained using frozen Gaussians from this trajectory extended to $t = 75$. The remaining inserts are eigenfunctions extracted from the frozen Gaussian dynamics.

but, if desired, real spectra may always be obtained by applying initial phase corrections. Substitution of (6.3) into (2.10) produces four terms, each one corresponding to one of the possible directions of motion of the wavepackets. Considering one of these terms we write

$$\begin{aligned}
 \langle q_x, q_y | \chi_m^{++} \rangle &= \sum_{n_x=-\infty}^{\infty} \sum_{n_y=-\infty}^{\infty} \int_{-\infty}^{\infty} dt \exp(-iE_m t / \hbar) \langle q_x | \psi_{q_{xt}+2n_x a_x, p_{xt}}^{(x)} \rangle \langle q_y | \psi_{q_{yt}+2n_y a_y, p_{yt}}^{(y)} \rangle \\
 &\propto \sum_{n_x=-\infty}^{\infty} \sum_{n_y=-\infty}^{\infty} \int_{-\infty}^{\infty} dt \\
 &\quad \times \exp \left[\frac{i}{\hbar} \left(\alpha_0 (q_x - q'_{xt})^2 + p_{x0} (q_x - q'_{xt}) + \frac{\pi \hbar m_x}{a_x} (q'_{xt} - q_{x0}) \right) \right] \\
 &\quad \times \exp \left[\frac{i}{\hbar} \left(\alpha_0 (q_y - q'_{yt})^2 + p_{y0} (q_y - q'_{yt}) + \frac{\pi \hbar m_y}{a_y} (q'_{yt} - q_{y0}) \right) \right] \quad (6.6)
 \end{aligned}$$

where

$$q'_{xt} = q_{x0} + p_{x0} t + 2a_x n_x \quad q'_{yt} = q_{y0} + p_{y0} t + 2a_y n_y. \quad (6.7)$$

If the trajectory is not periodic, then the trajectory covers all space evenly and all possible values of q'_{xt} and q'_{yt} are equally as likely. The double summation and time

integral in the above equation thus become a position space integral

$$\begin{aligned} \langle q_x, q_y | \chi_m^{++} \rangle &\propto \int_{-\infty}^{\infty} dq'_{xt} \exp \left[\frac{i}{\hbar} \left(\alpha_0 (q_x - q'_{xt})^2 + p_{x0} (q_x - q'_{xt}) + \frac{\pi \hbar m_x}{a_x} (q'_{xt} - q_{x0}) \right) \right] \\ &\times \int_{-\infty}^{\infty} dq'_{yt} \exp \left[\frac{i}{\hbar} \left(\alpha_0 (q_y - q'_{yt})^2 + p_{y0} (q_y - q'_{yt}) + \frac{\pi \hbar m_y}{a_y} (q'_{yt} - q_{y0}) \right) \right] \end{aligned} \quad (6.8)$$

which evaluates to give

$$\langle q_x, q_y | \chi_m^{++} \rangle \propto \exp [i\pi m_x (q_x - q_{x0}) / a_x + i\pi m_y (q_y - q_{y0}) / a_y] \quad (6.9)$$

and so a plane wave is produced. Combining the four terms from (6.3) and normalising results in

$$\langle q_x, q_y | \chi_m \rangle = 2(a_x a_y)^{-1/2} \sin(\pi m_x q_x / a_x) \sin(\pi m_y q_y / a_y) \quad (6.10)$$

and the exact eigenstates are obtained. Figure 4 shows some of the eigenstates obtained using frozen Gaussians from the extended trajectory shown in figure 3.

As a result of the sparseness of the rational numbers, the set of all trajectories that are periodic has measure zero. Thus, if the components of the momenta are selected at random then the probability of selecting a periodic trajectory is zero, and frozen Gaussian dynamics will give the correct eigenstates. When used in conjunction with the De Leon-Heller spectral quantisation method, the exact eigenvalues are also obtained. These arguments apply to a particle in any box for which the method of images can be applied.

Frozen Gaussian dynamics forces the energy spectrum obtained from (2.9) to be a convolution of evenly spaced lines, whereas for a particle in a box, the true energy spectrum is a convolution of quadratically spaced lines. Here, one would expect that only poor results could be obtained using frozen Gaussians, but the exact answer is recoverable. This example is somewhat specialised, but it does lend some insight into the success of the frozen Gaussian spectral quantisation method [14], and further investigation along these lines will be reported elsewhere [3, 34]. Frozen Gaussian dynamics is simple to use, being closely related to classical dynamics, yet it provides the exact solutions for these and other problems [4, 36]. It is becoming an important analytic [37] and computational [38] tool.

7. Conclusions

Gaussian wavepacket dynamics is shown to give the exact solutions to a fundamental problem of physics: a particle in a box. These results are important as they show that Gaussian wavepacket dynamics is capable of giving exact eigenfunctions for systems that have neither linearly spaced energy levels nor smooth potentials. Further, most of these problems are solvable exactly using the simpler frozen Gaussians and the De Leon-Heller spectral quantisation method [14], a method which is no more difficult to implement than is classical mechanics. Our analysis in terms of 'wrong dynamics with the right eigenfunctions' adds insight into the success of the frozen Gaussian method for calculating vibrational [14, 39, 40] and rotational [41, 42] wavefunctions. For the present case of bounded enclosures, the wavefunctions used are coherent states appropriate to the problem.

Acknowledgments

We thank the National Aeronautics and Space Administration, AMES Research Center, the National Science Foundation, Chemistry and the Office of Naval Research, Chemistry for providing the support which made this work possible.

References

- [1] Heller E J 1975 *J. Chem. Phys.* **62** 1544
- [2] Deutch J M, Kinsey J L and Silbey R 1970 *J. Chem. Phys.* **53** 1047
- [3] Reimers J R and Heller E J 1985 *J. Chem. Phys.* **83** 511
- [4] Reimers J R and Heller E J 1985 *J. Chem. Phys.* **83** 516
- [5] Thomson W 1847 *Br. Assoc. Adv. Sci. Rep.* **17** 6
- [6] Terras R and Swanson R A 1980 *Am. J. Phys.* **48** 526
- [7] Terras R and Swanson R A 1980 *J. Math. Phys.* **21** 2140
- [8] Magnus W 1974 *Non-Euclidean Tessellations and their Groups* (New York: Academic)
- [9] Turner J W 1984 *J. Phys. A: Math. Gen.* **17** 2791
- [10] Raszillier H 1984 *Quantum Mechanics on Fundamental Domains of Coxeter Groups* in press
- [11] Hiller H 1982 *Geometry of Coxeter Groups* (Boston: Pitman)
- [12] Bérard P H 1980 *Invent. Math.* **58** 179
- [13] Coxeter H S M 1974 *Regular Complex Polytopes* (Cambridge: Cambridge University Press)
- [14] De Leon N and Heller E J 1983 *J. Chem. Phys.* **78** 4005
- [15] Heller E J 1984 *Phys. Rev. Lett.* **53** 1515
- [16] Atkins P W 1970 *Molecular Quantum Mechanics* (Oxford: Clarendon) p 44
- [17] Louisell W H 1973 *Quantum Statistical Properties of Radiation* (New York: Wiley) p 104
- [18] McQuarrie D A 1976 *Statistical Mechanics* (New York: Harper and Row)
- [19] Reimers J R, Wilson K R and Heller E J 1983 *J. Chem. Phys.* **79** 4749
- [20] Marinov M S and Terentyev M V 1979 *Fortschr. Phys.* **27** 511
- [21] Jung C 1980 *Can. J. Phys.* **58** 58
- [22] Krishnamurthy H R, Mani H S and Verma H C 1982 *J. Phys. A: Math. Gen.* **15** 2131
- [23] Crandall R E 1983 *J. Phys. A: Math. Gen.* **16** 513
- [24] Korsch H J 1983 *Phys. Lett.* **97A** 77
- [25] Bérard P and Besson G 1980 *Ann. Inst. Fourier Grenoble* **30** 237
- [26] Berry M V 1983 *Chaotic Behaviour of Deterministic Systems* ed R Stora (Amsterdam: North-Holland) p 174
- [27] McDonald S W and Kaufman A N 1979 *Phys. Rev. Lett.* **42** 1189
- [28] De Leon N and Berne B J 1982 *Chem. Phys. Lett.* **93** 169
- [29] De Leon N and Berne B J 1982 *Chem. Phys. Lett.* **93** 162
- [30] Gutzwiller M C 1982 *Physica* **5D** 183
- [31] Gutzwiller M C 1983 *Physica* **7D** 341
- [32] Courant R 1918 *Math. Z.* **1** 321
- [33] Heller E J 1981 *J. Chem. Phys.* **75** 2923
- [34] Reimers J R and Heller E J 1986 *Justification of the De Leon-Heller spectral quantisation method: the one dimensional Morse oscillator* in preparation
- [35] Goldstein H 1950 *Classical Mechanics* (Reading, MA: Addison-Wesley) p 291
- [36] Herman M F and Kluk E 1984 *Chem. Phys.* **91** 27
- [37] Heller E J, Sundberg R L and Tannor D 1982 *J. Phys. Chem.* **86** 1822
- [38] Reimers J R, Wilson K R, Heller E J and Langhoff S R 1985 *J. Chem. Phys.* **82** 5064
- [39] Davis M J and Heller E J 1979 *J. Chem. Phys.* **71** 3383
- [40] Davis M J and Heller E J 1981 *J. Chem. Phys.* **75** 3916
- [41] Blanco M and Heller E J 1983 *J. Chem. Phys.* **78** 2504
- [42] Blanco M and Heller E J 1985 *J. Chem. Phys.* to be published